OXIDE EUTECTICS: ROLE OF INTERFACES IN THE MATERIAL PROPERTIES[*]

V. M. Orera, R. I. Merino, J. A. Pardo, A. Larrea, G.de la Fuente, L. Contreras, J. I. Peña
Instituto de Ciencia de Materiales de Aragón, C.S.I.C.- Universidad de Zaragoza,
50009 - Zaragoza, Spain

Eutectics are a paradigm of micron scale composite materials with improved properties. Improved mechanical properties and thermal stability of eutectics as compared with ceramics or single crystals of component phases are a consequence of the presence of huge amounts of interfaces. Interface morphology and ordered structures also invites to explore other properties of regular eutectics such as light guiding effects, anisotropic ion conduction, use as structured substrates for patterned films, etc. In this work we report on the production of several eutectic crystals of wide band gap materials, grown from the melt by unidirectional solidification. The structure, mechanical properties and interface morphology were determined using different techniques including X-ray diffraction, SEM, TEM, Raman and optical spectroscopy techniques. Examples of lamellar microstructures are provided by the ZrO_2-CaO, ZrO_2-NiO and CaF_2-LiF systems. Planar light guiding and anisotropic ion conduction are some of the unconventional properties of these regular composites. ZrO_2-MgO, ZrO_2-Al_2O_3 and CaF_2-MgO are examples of fibrous eutectics. The alumina-zirconia composite presents excellent mechanical properties also related to the presence of residual thermostresses that have been measured using different piezospectroscopic effects. The fluorite-magnesia eutectic is an example of semifaceted non-regular composite showing light guiding effects.

PACS: 81.10.-h, 81.40.Np, 81.40.Tv

1   Introduction

In composites phase distribution, size, and shape as well as the interface characteristics and density play a crucial role in determining the properties of the materials. New or improved properties are often obtained through the development of novel microstructures. Eutectics are a paradigm of materials with a very fine microstructure (interparticle spacing $\lambda \approx 0.5 - 10$ μm) which may combine the characteristics of each constituent to optimize the physical properties [1,2]. Interfacial area density is also very large in these materials (about 10^6 m^{-1}). The reduced interspacing distance hinder the presence of large defects in the as-grown materials. Consequently, eutectics show excellent mechanical properties at room temperature and good retention of these properties up to temperatures near to the melting point, as it has been previously reported [3]. Directional solidification growth may produce regular eutectics with ordered microstructures [4]. The basic

---

[*]Presented at the Workshop on Solid State Surfaces and Interfaces II, Bratislava, Slovakia, June 20 – 22, 2000.

microstructure of a regular eutectic consists of either single crystal rods or lamellae embedded in a single crystal matrix. In the simplest case of isotropic surface energy, fibres instead of lamellae are found for volume fraction of the minority phase less than 28%. The interparticle spacing λ depends on the solidification rate R as $\lambda^2 R = \text{const}$ [5].

Recently, research in non-metallic eutectics has been promoted by their interesting properties. For example, some oxide eutectic materials can be used as oxygen conductors with a mass density alike that of single crystals but a better mechanical and thermal stress resistance [6]. Moreover, step refractive index profiles derived from the interface morphology and the ordered microstructure also invites to explore their optical properties. For instance, planar optical waveguiding was reported in ZrO_2-CaO regular eutectics [7] and CaF_2-MgO eutectic can be viewed as a bunch of optical fibers with a density of 40000 fibers/mm^2 [8]. From the point of view of optical spectroscopy, these materials present the unusual characteristics of monolithic multiphase materials with different environments for optically active ions as it has been reported for ZrO_2-CaO eutectics activated with Er^{3+} ions [9].

In this paper we collect the preparation procedures and results of the microstructure studies in a number of wide-band-gap eutectic crystals grown from the melt by two different directional solidification procedures, the Laser Floating Zone method (LFZ) and the conventional Bridgman method. The unique characteristics of the microstructures and interfaces are discussed in the light of the processing parameters and phase properties. Some remarkable relationships between microstructure and properties are briefly discussed.

2   Experimental details

The composition and melting temperature of the six eutectics studied are given in Tab. 1. Precursor rods, 1 to 2 mm in diameter and 50 to 100 mm in length, were prepared from the powder mixture of the high melting temperature eutectic oxides ZrO_2-CaO, ZrO_2(CaO)-NiO, Al_2O_3-ZrO_2(Y_2O_3) and ZrO_2-MgO by pressureless sintering at 1500 °C. Directionally solidified eutectic fibers were then produced from the precursor fibers by the laser, floating zone-method, as described elsewhere [10]. The solidification rate was varied between 10 and 100 mm/h. The CaF_2-MgO and CaF_2-LiF eutectics were grown by the Bridgman method in a radio-frequency heated furnace using vitreous carbon crucibles in Ar inert atmosphere at a rate of 5 mm/h. Samples of cylindrical shape of 1.7 cm^2 × 10 cm size were obtained.

Compound	Melting point (°C)	Composition (wt)
ZrO_2-CaO	2250	$0.6\,CaZrO_3 + 0.4\,Ca_{0.25}Zr_{0.75}O_{1.75}$
ZrO_2-MgO	2170	$0.25\,MgO + 0.75\,Mg_{0.2}Zr_{0.8}O_{1.8}$
ZrO_2(CaO)-NiO	1700	$0.6\,NiO + 0.4\,Ca_{0.15}Zr_{0.85}O_{1.85}$
ZrO_2-Al_2O_3	1860	$0.47\,ZrO_2 + 0.53\,Al_2O_3$
CaF_2-LiF	780	$0.46\,CaF_2 + 0.54\,LiF$
CaF_2-MgO	1350	$0.9\,CaF_2 + 0.1\,MgO$

Tab. 1. Composition and melting temperature of the eutectics studied.

The samples were cut and polished with diamond paste for optical measurements and for

morphological evaluation in the scanning electron microscope. No differential polishing of the phases was observed.

The crystal structure of the eutectic phases was determined by XRD, Scanning (SEM) and Transmission Electron Microscopy (TEM) and micro-Raman techniques and the chemical composition by EDX analysis. The microstructure of the samples was studied by Optical Microscopy as well as SEM and TEM. The SEM experiments were performed in a Jeol 6400 apparatus equipped with a Link Analytical Energy Disperse Spectroscopy (EDS) analyzer. The TEM experiments were carried out in a Jeol 2000FXII microscope also equipped with a Link Analytical EDS analyzer.

The Cr^{3+} luminescence and the Raman dispersion measurements were performed in back-scattering geometry using an optical microprobe spectrometer (DILOR XY, Lille, France) with a diode array multichannel detector. The emission and the Raman dispersion of selected areas can be measured simultaneously with this equipment. A region of about 1 μm diameter and 4 μm in depth can be analyzed using 100× objective lens and 400 μm field aperture in the image focal plane. Further details of the piezospectroscopic experiments are given elsewhere [11].

The conductivity measurements were performed in bars of a typical size of $S \times l = 3 \times 4$ or slices of about 4×0.2 mm^3 contacted with Pt paste electrodes in air or a flowing N$_2$ atmosphere using a Schulmberger 1260 impedance analyzer.

3 Experimental results

3.1 Microstructure

The microstructure of the eutectic samples was studied by optical and electron microscopy. It depends to some extent on crystal growth conditions such as solidification gradients, impurity content, solidification rate, etc. For the lamellar eutectics the microstructure is as follows: ZrO$_2$-CaO presents well-ordered regions of alternating calcium-stabilized-zirconia (CSZ see Tab. 1) and CaZrO$_3$ (CZO) single crystal lamellae a few microns thick [12]. CaF$_2$-LiF grows in the form of lamellae of CaF$_2$ (about 3 μm thickness) and LiF (about 2 μm).

In the case of ZrO$_2$-NiO eutectic, the size of ordered grains is larger (see Fig. 1a) and it also consists of alternating CSZ (see Tab. 1 for composition) and NiO lamellae. Thermal treatments in a reducing atmosphere produces the reduction of NiO to metallic Ni. The new microstructure consists of Ni metallic particles of the order of few microns size alternating with pores inside the CaSZ eutectic skeleton (Figs. 1b and 1c). The reduced sample presents metallic electric conduction besides the ionic one.

Fibrous ZrO$_2$-MgO consists of grains with a nearly hexagonal array of MgO fibers about 1 μm diameter embedded in a single crystal matrix of magnesia-stabilized-zirconia (MgSZ, see Tab. 1 for composition). Under certain conditions ZrO$_2$-MgO eutectic can be grown in the form of lamellae. Al$_2$O$_3$-ZrO$_2$ eutectics can be grown in the form of either well ordered colonies with hexagonal array of ZrO$_2$ fibers of 0.3 μm diameter, 60 μm long in the Al$_2$O$_3$ matrix (samples ZAI Fig. 1a in [11]) or disordered colonies. Doping with Y$_2$O$_3$ (samples ZAII) reduces the colony size and in some conditions an homogeneous microstructure consisting of an interpenetrating network of yttria- stabilized-zirconia (YSZ) and Al$_2$O$_3$ is obtained [11]. The CaF$_2$-MgO eutectic contained single crystal MgO fibres (0.5-0.8 μm size) arranged in a CaF$_2$ matrix [8]. The matrix is formed of CaF$_2$ grains (~ 400 μm size) crystallographically misaligned $\sim 1 - 2°$ from one

(a)

(b)

(c)
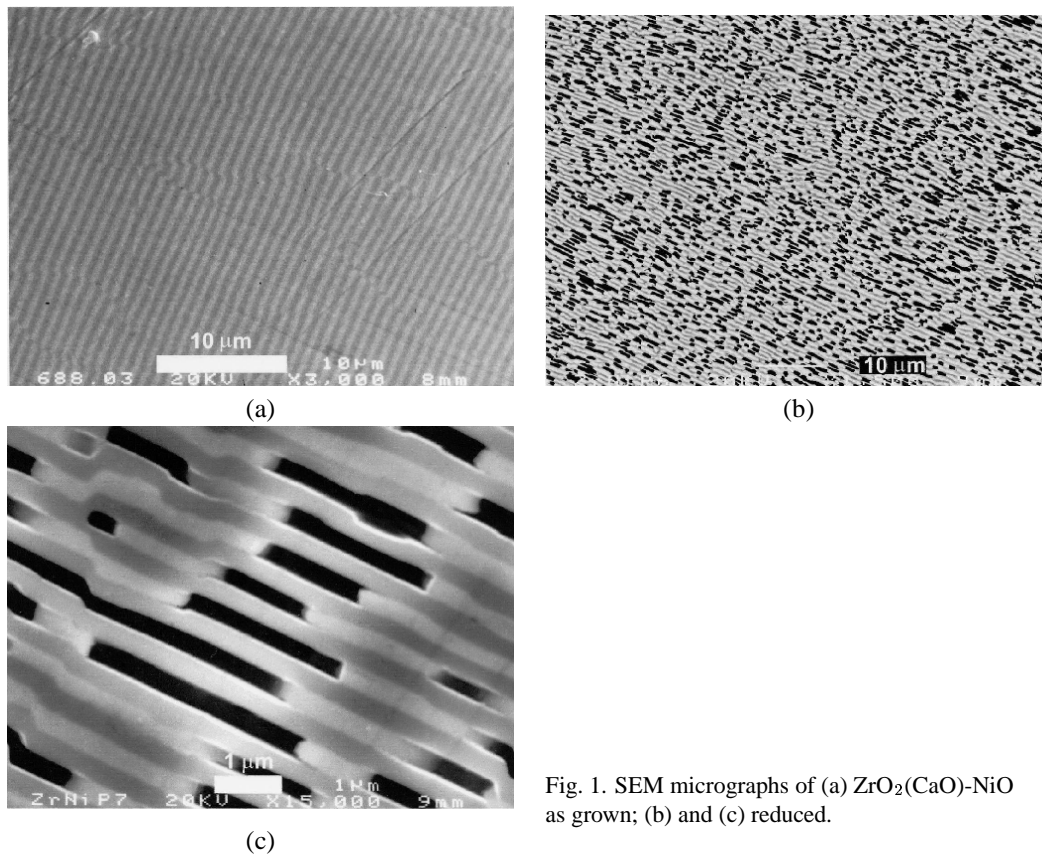
Fig. 1. SEM micrographs of (a) ZrO$_2$(CaO)-NiO as grown; (b) and (c) reduced.

another, whereas the fibres ($\sim$ 400 μm length) are distributed in a nearly hexagonal array (fibre spacing 6-8 μm). The MgO fibres were found to be discontinuous at the grain boundaries.

Crystal growth morphology can be predicted using the entropy of fusion criterion of Hunt and Jackson (HJ) [13]. For $\Delta S_f/R > 2$, ΔS_f being the fusion entropy (latent heat / fusion temperature) and R the gas constant, the interfaces are expected to be faceted, the growth is anisotropic and along low-index Miller faces. On the contrary, for $\Delta S_f/R < 2$ the interfaces are non-faceted. In Tab. 2 we give the molar entropy of fusion for the component phases. Tendency for eutectic growth is the following: low fusion entropy leads to coupled growth of component phases, the undercooling is expected to be low and solidification proceeds with an isothermal front. In such a case the morphology of the eutectic is generally regular. On the contrary if fusion entropies are large the component phases grow anisotropically, facets are developed and the growth of the phases is not coupled. This situation produces irregular eutectics.

CaF$_2$-LiF eutectic follows this criterion. Fusion entropies are low, morphology is regular and lamellae are not faceted (see Fig. 2). CaF$_2$-MgO eutectic is in the middle as the low fusion entropy of the fluorite might partially compensate the high value for MgO and so explain the semifaceted shape of MgO fibres [8]. The opposite is the case of alumina-zirconia eutectics.

Compound	n^{**}	$\Delta S_f/R$	Space Group
ZrO_2^*	2.19	3.5	O_h^5, C_{2h}^5
Al_2O_3	1.76	5.7	D_{3d}^6
NiO	2.18	2.7	O_h^5
MgO	1.75	3	O_h^5
LiF	1.39	1	O_h^5
CaF_2	1.44	2.1	O_h^5
$CaZrO_3$	2.15	***	D_{2h}^{16}

* Similar values for other zirconia compositions. ** For λ = 550 nm. *** No data available.

Tab. 2. Crystal structure, refractive index n and adimensional fusion entropy $\Delta S_f/R$ of component phases.

Fusion entropy of Al_2O_3 is high and alumina crystal growth governs the eutectic morphology which consists of Al_2O_3 faceted single crystals with ZrO_2 fibres non-regularly distributed. In the other zirconia compounds tendency is for coupled growth giving non-faceted regular eutectics but some faceting is observed for the ZrO_2-NiO eutectic. The orientation relationships between component phases and interface morphology for the systems studied are collected elsewhere [14].

3.2 Mechanical properties

The mechanical properties of several eutectics were measured on cylindrical rods using the experimental procedures reported elsewhere [14]. The results of the mechanical characterization of the eutectic compounds are summarized in Tab. 3. The first interesting result is the elevated elastic moduli of the materials. This is indicative of an excellent bonding between the different phases in the eutectics and of the absence of porosity or cracks in the microstructure. From the point of view of strength and toughness, the mechanical properties of CaSZ-$CaZrO_3$ and MgSZ-MgO eutectics were not especially remarkable. This is not the case, however, for the Al_2O_3-$ZrO_2(Y_2O_3)$ rods, which presented exceptional values of strength, combined with an excellent toughness. Sayir *et al.* found similar values for the tensile strength of Al_2O_3-$ZrO_2(Y_2O_3)$ fibres processed by the laser floating zone method [3]. These authors also studied the high-temperature strength and creep resistance; they concluded that the combination of strength, toughness, and thermal expansion coefficient of these fibers was very promising to be used as reinforcement in intermetallic and metal- matrix composites.

The excellent strength and toughness of this eutectic composite has to be found in the peculiar characteristics of its microstructure. Firstly, eutectic composites produced by directional solidification exhibit a defect-free fine microstructure, which limits the size of defects, being smaller than the critical defect size. In addition, thermal residual stresses develop in the eutectic rods upon cooling from the processing temperature as a result of the mismatch in thermal expansion coefficients between both phases [15] as well as phase transformation. The residual stresses in Al_2O_3-ZrO_2 and Al_2O_3-$ZrO_2(Y_2O_3)$ eutectics were measured by means of the piezospectroscopic effect in the R- lines luminescence of Cr^{3+} in Al_2O_3, whose maxima exhibit a marked shift with stress [16]. This allows to compute the stress state in the alumina phase. The results show that the alumina was in compression in the ZAII eutectic rods (mean hydrostatic stress -0.36 GPa) and in tension in the ZAI material (mean hydrostatic stress 1.13 Gpa) [11]. The

	Eut. ZrO$_2$-CaO	Eut. MgO-ZrO$_2$	Eut. Al$_2$O$_3$-YSZ	YSZ (ceram.)	SiC	Alumina
Young's Modulus (GPa)	220	285	343	150	420	390
Flexural Strength (MPa)	220	300	1130	240	210-380	330
Fracture toughness K$_{IC}$ (MPam$^{1/2}$)	—	1.2	7.8	5	4	3.5
Thermal Expansion Coef. ($\times10^{-6}$ deg^{-1})	10	—	8.1	10	4.5	8.0
Thermal cond. (W/mK)	2	—	—	2	90-160	30
Maximum use temperature ($^\circ$C)	2200	2100	1700	2200	1650	1700
Thermal shock resistence	Excel.	Excel.	Excel.	Good	Excel.	Good

Tab. 3. Physical properties at room temperature of some oxide eutectics compared with some common materials.

opposite nature of the residual stresses was attributed to the presence of a phase transformation (from tetragonal to monoclinic) in the Al$_2$O$_3$-ZrO$_2$ (ZAI) composite. This phase transformation did not occur in the Al$_2$O$_3$-ZrO$_2$(Y$_2$O$_3$) (ZAII) rods, which were stabilized by the presence of yttria. In fact, the Raman spectra of both eutectics only showed the peaks of the monoclinic phase in the former and of the tetragonal phase in the latter. Cubic zirconia was not detected in either material.

The large compressive residual stresses in the alumina phase of the Al$_2$O$_3$-ZrO$_2$(Y$_2$O$_3$) rods contributed actively to increase its strength. Alumina is the brittle phase in the composite, while stabilized tetragonal ZrO$_2$ forms the tough component with a higher resistance to crack initiation and propagation. Failure is thus likely to start in the alumina phase but this requires to overcome the compressive residual stresses.

Another example of toughening in eutectic compounds was found in CaF$_2$-MgO system. Matrix cracks do not penetrate into the MgO fibres but they are deflected along the fiber/matrix interface [8]. Thermoelastic stresses in this composite are expected to be very small and crack deflection is due to the differences in toughness between MgO and CaF$_2$. The elastic energy stored in the fibres, together with the energy spent pulling out the fibres which are eventually broken within the matrix, increase significantly the fracture energy of the composite. In fact, the resistance to cleavage of the eutectic crystals involving CaF$_2$ was much higher than that of CaF$_2$ single crystals.

3.3   Optical properties

Except for NiO all the component phases are wide band gap compounds exhibiting a broad transparency window from 0.2 to 10 μm. As grown ingots are optically translucent due to the

Eutectic	Guiding phase	Shape	Size (μm)	V	λ_c (μm)
ZrO_2-CaO	$Ca_{0.25}Zr_{0.75}O_{1.75}$	Planar	2	5.2	1.7
Al_2O_3-ZrO_2	ZrO_2	Fibre	0.3	2.45	0.5
CaF_2-MgO	MgO	Fibre	1.2	7.5	1.6
LiF-CaF_2	CaF_2	Planar	2	1.8	0.6

Tab. 4. Waveguide parameter V for $\lambda = 0.5$ μm. and cut-off wavelength of some eutectic systems

refractive index contrast between eutectic components. Depending on this index contrast the materials light transmitance ranges from very low values for highly dispersive compounds such as ZrO_2-Al_2O_3 eutectics to nearly unity for the transparent LiF-CaF_2 eutectics.

Moreover, ordered structures with periodicity of the order of the light wavelength added to the refractive index contrast between phases leads to diffraction, interference, polarization effects, etc., which can be used in the development of optical systems [17]. Here we will focus on the light guiding effect in some eutectic systems.

Taking the refractive index given in Tab. 2 we can calculate some fibre parameters for these systems. This waveguide parameter V defined as [18]

$$V = \frac{2\pi}{\lambda}d\left[n_i^2 - n_o^2\right]^{\frac{1}{2}} \tag{1}$$

where λ is the light wavelength in the vacuum, d is the guide size parameter which is the fibre radius for cylindrical fibers and half the lamella thickness for planar waveguides. n_i and n_o the refractive index of the waveguide and surrounding medium, respectively.

The number of modes propagating in the guide depends on V. Single-mode operation is obtained for

$$\lambda \geq \lambda_c = 4d\left[n_i^2 - n_o^2\right]^{\frac{1}{2}} \qquad \text{for lamellae}$$

and

$$\lambda \geq \lambda_c = \frac{2\pi d}{2.405}\left[n_i^2 - n_o^2\right]^{\frac{1}{2}} \qquad \text{for fibres}$$

with λ_c being the cut-off wavelength for the most energetic light propagating in single-mode form.

From the refractive index values of Tab. 2 light guiding effects are expected in CSZ lamellae in the ZrO_2-CaO eutectic, in CaF_2 lamellae in CaF_2-LiF eutectic, in ZrO_2 fibres in the ZrO_2-Al_2O_3 system and in MgO fibres in the CaF_2-MgO eutectic. Planar optical waveguiding has been previously reported in the ZrO_2-CaO eutectic [7]. The waveguide parameters for those systems are given in Tab. 4. It can be concluded that single-mode operation in the third optical window is predicted for ZrO_2-CaO and CaF_2-MgO eutectics. For the ZrO_2-Al_2O_3 and LiF-CaF_2 systems the cut-off wavelength decreases down to visible optical range.

In Fig. 2 we present an optical micrograph taken in the transmission mode through a slab of 2 mm thick of the LiF-CaF_2.
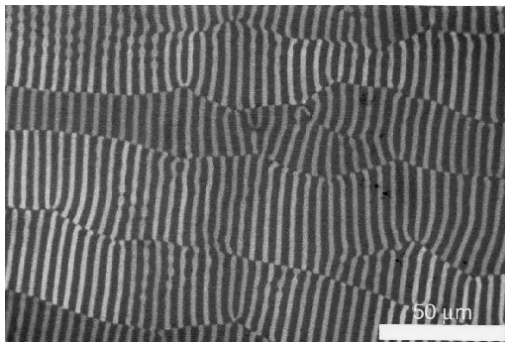
Fig. 2. Transmission optical microscope image of LiF-CaF$_2$ platelet of 2 mm thickness.
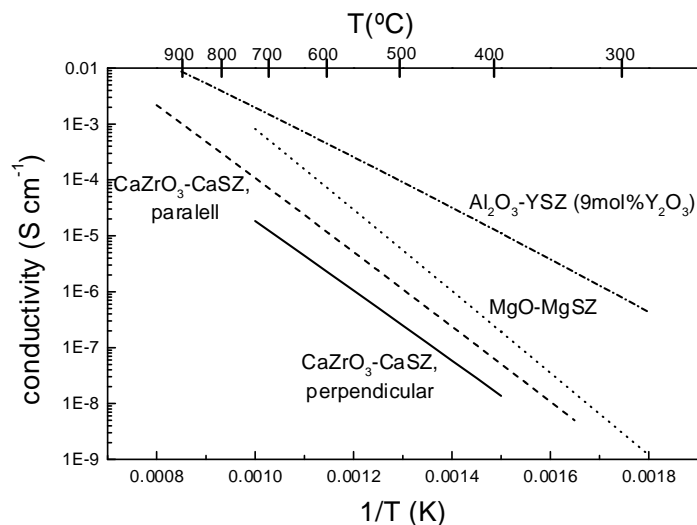
Fig. 3. DC conductivity data of the zirconia based eutectic samples.

3.4 Electrical conductivity

Stabilized zirconia is perhaps the most widely used oxygen electrolyte. Most of the eutectic systems studied by us consist of combinations of an ionic conductor with an insulator. In Fig. 3 we summarize the conductivity measurements as a function of temperature for zirconia based eutectics. The best ionic conductor is Al$_2$O$_3$-YSZ. Conductivity values are close to those predicted from the effective medium approximation for the disordered case [19].

For lamellar compounds a strong anisotropy is predicted. The conductivity measured with the electric field either parallel or perpendicular to the lamellae should be $\sigma_\parallel \approx f\sigma_1$ and zero respectively as it has been observed in the case of CSZ-CZO eutectic [5]. For fibrous compounds there are always conduction paths and such anisotropy is not observed.

Electrical behavior of the ZrO$_2$-NiO eutectic is different as it is dominated by the semiconducting characteristics of the NiO. Interestingly, this eutectic can be transformed by reduction to

a composite of metallic Ni + pores inside a lamellar skeleton of zirconia. The compound presents metallic conduction and pores and it can be a good candidate for anode material for oxide fuel cells.

4 Conclusions

The exceptional microstructure and interface morphology of eutectic crystals of ionic compounds opens a broad scope of possible applications besides those derived from mechanical properties. From the point of view of optical applications light guiding by fibres or lamellae can be used in face plates and other devices. The main limitation for practical use comes out from the small size of eutectic grains which makes it difficult the necessary connectivity between guides. In the case of electrical applications the materials are very interesting because of their toughness and thermal shock resistance in spite that the electrical conductivity is lower than for monophasic compounds.

References

[1] C. De Rosa, Ch. Park, E.L. Thomas, B. Lotz: *Nature* **405** (2000) 433

[2] Y. Waku, N. Nakagawa, T. Wakamoto, H. Ohtsubo, K. Shimizu, Y. Kohtoku: *Nature* **389** (1997) 49

[3] A. Sayir, S.C. Farmer, P.O. Dickerson, H.M. Yun: *Mat. Res. Soc. Symp. Proc.* **365** (1995) 21

[4] W. Kurtz, D.J. Fisher: *Fundamentals of Solidification*, Trans. Tech. Publications, 1992

[5] R.L. Ashbrook: *J. Am. Ceram. Soc.* **60** (1977) 428

[6] R.I. Merino, J.I. Peña, V.M. Orera, G.F. de la Fuente: *Solid State Ionics* **100** (1997) 313

[7] V.M. Orera, J.I. Peña, R.I. Merino, J.A. Lázaro, J.A. Vallés, M.A. Rebolledo: *Appl. Phys. Lett.* **71** (1997) 2746

[8] A. Larrea, L. Contreras, R.I. Merino, J. Llorca, V.M. Orera: *J. Mater. Res.* **15** (2000) 1314

[9] R.I. Merino, J.A. Pardo,J.I. Peña, G.F. de la Fuente, A. Larrea, V.M. Orera: *Phys. Rev. B* **56** (1997) 10907

[10] G.F. de la Fuente, J.C. Diez, L.A. Angurel, J.I. Peña, A. Sotelo, R. Navarro: *Adv. Mater.* **7** (1995) 10853

[11] J.A. Pardo, R.I. Merino, V.M. Orera, J.I. Peña, C. González, J.Y. Pastor, J. Llorca: *J. Am. Ceram. Soc.* **83** (2000) in print

[12] J.I. Peña, R.I. Merino, G. de la Fuente, V.M. Orera: *Adv. Mater.* **8** (1996) 909

[13] J.D. Hunt, K.A. Jackson: *Trans. AIME* **236** (1966) 843

[14] V.M. Orera, R.I. Merino, J.A. Pardo, A. Larrea, J.I. Peña, C. González, P. Poza, J.Y. Pastor, J. Llorca: *Acta Materialia* (2000) in print

[15] W.D. Kingery, H.K. Bowen, R.D. Uhlmann: *Introduction to Ceramics*, 2nd edition, John Wiley & Sons, New York, 1976

[16] J. He, D.R. Clarke: *J. Am. Ceram. Soc.* **78** (1995) 1347 ; J. He, D.R. Clarke: *Proc. R. Soc. A* **453** (1997) 1981

[17] J.D. Parsons, A.S. Yue: *J. Cryst. Growth* **55** (1981) 470

[18] A.W. Snyder, J.D. Love: *Optical Waveguide Theory*, Chapman and Hall, 1983

[19] D. Stroud: *Phys. Rev. B* **12** (1975) 3368